Article ID: 1000 - 8152(2001)06 - 0871 - 05

Fuzzy and Robust Control System of Intelligent RLED Arm Manipulators for Dynamic Obstacles

WEI Wu
(Department of Road and Traffic Engineering, Changsha Communications University · Changsha, 410076, P.R.China)
Jean Bosco Mbede and HUANG Xinhan
(Department of Control Science and Engineering, Huazhong University of Science and Technology · Wuhan, 430074, P.R.China)

Abstract: This paper presents a fuzzy and robust close loop control system for nonlinear electromechanical systems of an electric motor actuating an arm robot. This control system is applied to the three basic navigation problems of intelligent robot systems in unstructured environments: autonomous planning, fast nonstop navigation without collision with obstacles, and dealing with structured and/or unstructured uncertainties. The stability of close loop control system is guaranteed by Lyapunov theory.

Key words: fuzzy & robust motion control; RLED arm manipulators; dynamic obstacles
Document code: A

智能 RLED 动态目标中机器手的模糊鲁棒控制系统

魏　武　　Jean Bosco Mbede　黄心汉
(长沙交通学院道路与交通工程系·长沙,410076)　(华中科技大学控制科学与工程系·武汉,430074)

摘要: 给出了一种电机驱动机器手中非线性机电模型的模糊鲁棒闭环控制系统,此控制系统可处理非结构环境下的三个主要的智能机器人导航问题:自动化规划、快速连续导航中的避障、处理结构和(或)非结构不确定性.

关键词: 模糊和鲁棒运动控制; RLED 机器手; 动态目标

1 Introduction

One of the fundamental characteristics of an autonomous, intelligent robot system is its ability to move without collision in unstructured environments with little a priori information. In most cases where the research on the applications of nonlinear control theory to the motion control of robots, the actuator dynamics have been excluded from the dynamic models of robot arms[1-7]. As pointed out by Tarn. et al[7], adding actuator dynamics can improve the performance of motion controllers. The robot-plus-actuator system is also called rigid-link electrically driven (RLED) robot system.

This paper presents a fuzzy and robust system to control the motion of robot manipulators. In this system, a robust fuzzy obstacle avoidance scheme could deal with structured and/or unstructured uncertainties, and moving obstacles. A robust controller is designed to compensate for nonlinearities in robot-plus-actuator dynamics, robust fuzzy control, and local path planning methods. We aim to achieve fast, robust and continuous sensor guidance of intelligent robots in dynamic environments with moving obstacles.

2 RLED robot model and its properties

For simplicity, we consider robot manipulators driven by armature-controlled direct-current motors with voltages being input to amplifiers. It should be noted that the following analysis could also be extended to other motors commonly used in robotics, such as brush direct-current motors.

The voltage equation of the armature circuit of the motor of the robot arm is given by Tarn.et al as

$$RI + L\dot{I} + K_e\dot{W} + u_d = u_e, \tag{1}$$

where $I, \dot{I} \in \mathbb{R}^n$ is the armature current and its first derivative to time, respectively, $R \in \mathbb{R}^n$ is the resistance of armature circuit, $L \in \mathbb{R}^{n\times n}$ is a positive definite constant diagonal matrix denoting the electrical inductance, K_e is the electric potential constant of motor, $W \in \mathbb{R}^n$ is the angular position of rotor, $W = N_q$(q denote the an-

Received date: 2000 - 03 - 10; Revised date: 2001 - 04 - 02.

gular position of joint, N is the gear ratio of the joint), $u_d \in \mathbb{R}^n$ represents the voltage disturbance, and $u_e \in \mathbb{R}^n$ is the armature voltage.

Since the torque of motors is positive proportional to electromagnetism and armature current, the joint torque $\tau \in \mathbb{R}^n$ is then

$$\tau = NK_T I, \tag{2}$$

where $K_T \in \mathbb{R}^{n\times n}$ is the constant matrix of torque, which characterizes the electromechanical conversion between current and torque.

There are uncertainties in (1) and (2). We assume the following bounds on the uncertainties:

Assumption 2.1 The torque transmission matrix K_T is bounded by

$k_1 \| x \|^2 \leqslant x^T K_T x \leqslant k_2 \| x \|^2$,

for an $n \times 1$ state vector x to this given system,

(3)

where k_1 and k_2 are positive scalar bounding constants.

Assumption 2.2 The inductance matrix L is bounded by

$l_1 \| x \|^2 \leqslant x^T L x \leqslant l_2 \| x \|^2$,

for an $n \times 1$ state vector x to this given system,

(4)

where l_1 and l_2 are positive scalar bounding constants.

Having obtained the actuator equations, we consider now the dynamic equations of robot manipulator links which are well understood (see e.g.[5,6]) and are given by

$$M(q)\ddot{q} + C(q,\dot{q})\dot{q} + G(q) + F(\dot{q}) + \tau_d = \tau = NK_T I, \tag{5}$$

where $q, \dot{q}, \ddot{q} \in \mathbb{R}^n$ denote the angular vectors of link position, velocity, and acceleration, respectively, $M(q) \in \mathbb{R}^{n\times n}$ is the inertia matrix, $C(q,\dot{q}) \in \mathbb{R}^n$ is the Coriolis and centrifugal torque vector, $G(q) \in \mathbb{R}^n$ is the gravitational torque vector, $F(\dot{q}) \in \mathbb{R}^n$ represents the friction torque vector, and $\tau_d \in \mathbb{R}^n$ is the vector of any generalised input due to disturbances or unmodeled dynamics.

There are uncertainties in $M(q)$ and $C(q,\dot{q})$ due to the unknown load on the manipulator. We assume the following bounds on the uncertainties:

Property 2.1 Boundedness of the inertia matrix (Strictly speaking boundedness of the inertia matrix requires in general that all joints be revolute.):

The inertia matrix $M(q)$ is symmetric and positive definite, and satisfies the following inequalities:

$$m_1 \| \dot{q} \|^2 \leqslant \dot{q}^T M(q) \dot{q} \leqslant m_2 \| \dot{q} \|^2, \dot{q} \in \mathbb{R}^n, \tag{6}$$

where m_1 and m_2 are known positive constants and $\| \cdot \|$ denotes the standard Euclidean norm.

Assumption 2.3 There exist $C_0(q,\dot{q})$($C_0(q,\dot{q})$ is obtained by the maximum value $m_{p_{\max}}$ of payload), and a nonnegative function $C_1(q,\dot{q})$ such that

$$\| C(q,\dot{q}) - C_0(q,\dot{q}) \| \leqslant C_1(q,\dot{q}). \tag{7}$$

To facilitate control system design, the following property[8] can be exploited:

Property 2.2 Skew symmetry:

The inertia and centripetal-Coriolis matrices have the following property:

$$\dot{q}^T(\dot{M}(q) - 2C(q,\dot{q}))\dot{q} = 0, \ \dot{q} \in \mathbb{R}^n, \tag{8}$$

where $\dot{M}(q) - 2C(q,\dot{q})$ is a skew symmetric matrix.

3 Robot control design

In this section, we develop an assembled robust fuzzy controller for inexact RLED model knowledge given by (1) and (3) to accomplish a certain motion to reach the prescribed goal X_d. The trajectory of the robot is not known or calculated in advance. To accomplish this task, we first define $a(t) \in \mathbb{R}^n$ as $a = -\dot{q}$. With regard to differentiating (8) and invoking (3), it is seen that the robot dynamic links are expressed in terms of a as[9]

$$M(q)\dot{a} = -C(q,\dot{q})a + G(q) + F(\dot{q}) + \tau_d - \tau. \tag{9}$$

Adding and subtracting $M_0(q)\dot{a}$ and $C_0(q,\dot{q})a$ yields

$$M_0(q)\dot{a} = -C_0(q,\dot{q})a + f_1(x_1) + \tau_d - \tau, \tag{10}$$

where, $M_0(q)$ is the maximum value of $M(q)$, the nonlinear function $f_1(x_1)$ which contains the imperfectly known and difficult to determine robot parameters is defined as

$$f_1(x_1) = (M_0(q) - M(q))\dot{a} + (C_0(q,\dot{q}) - C(q,\dot{q}))a + G(q) + F(\dot{q}). \tag{11}$$

The vector x_1 required to compute $f_1(x_1)$ can be defined as

$$x_1 = [a^T \quad \dot{a}^T \quad q^T \quad \dot{q}^T], \tag{12}$$

which can be measured.

Now let I_d be a value of I that stabilizes the dynamics

(10) in the form

$$M_0(q)\dot{a} = -C_0(q,\dot{q})a+f_1(x_1)+\tau_d-NK_TI_d+NK_T\eta \tag{13}$$

with

$$\eta = I_d - I, \tag{14}$$

an error term of armature current. Signal $I_d(t)$ will be selected later. To find the complete error dynamics, differentiate L_η and substitute from (1) to find[9]

$$L\dot{\eta} = f_2(x_2) + u_d - u_e, \tag{15}$$

where the unknown nonlinear motor function is

$$f_2(x_2) = RI + L\dot{I}_d + NK_e\dot{q}. \tag{16}$$

One may select x_2 as

$$x_2 = [I^T \quad \dot{I}_d \quad \dot{q}]. \tag{17}$$

Fig. 1 shows the structure of the proposed control strategy. It is important to note that there is one controller at each joint. The robot is controlled directly in Cartesian space, also called Workspace (W-space). In comparison to potential fields using analytic functions, the advantage of this control strategy is to avoid the so-called "inverse kinematics" (which is the inverse processing of "forward kinematics") problem in robotics, the "robot term" is described by expression (19).

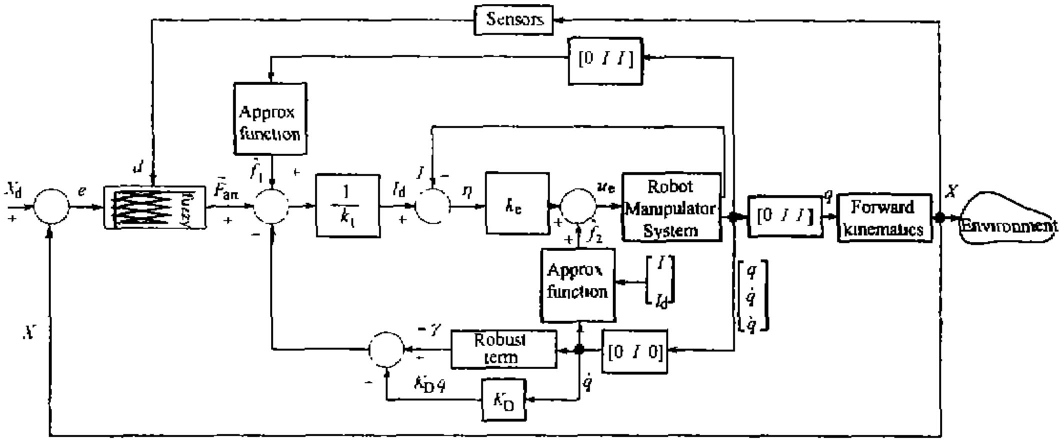

Fig. 1 Controller structure

3.1 Robust control

A suitable approximation-based controller is given by the desirable value of armature current as

$$I_d = \frac{1}{K_1}(\hat{f}_1 + k_D a + \bar{F}_{art} + \gamma_1) \tag{18}$$

with $\hat{f}_1(x_1)$ an estimate of the unknown robot function $f_1(x_1)$ (see [9]). $\bar{F}_{art}$ is an artificial force (see [10]), provided by the fuzzy controller. The robustifying signal $\gamma_1(t)$ is required to compensate for the mismatch between $\hat{f}_1(x_1)$ and $f_1(x_1)$, and is defined as

$$\gamma_1 = \frac{a\rho_1^2}{\| a \| \rho_1 + \varepsilon_1}, \tag{19}$$

where ε_1 is small, a positive constant controller gain, the bounding positive scalar function ρ_1 is defined as

$$\rho_1 > \| \tilde{f}_1 \| = \| f_1 - \hat{f}_1 \|, \tag{20}$$

where the function approximation error $\tilde{f}_1$ is given by

$$\tilde{f}_1 = f_1 - \hat{f}_1. \tag{21}$$

Substituting (18) into the open loop dynamics of (10), the closed-loop system becomes

$$M_0(q)\dot{a} = -[K_D + C_0(q,\dot{q})]a+\tilde{f}_1(x_1)-\bar{F}_{art}+\tau_d+\gamma_1. \tag{22}$$

The second step is the design of the voltage control u_e for the open loop system of (15). The control input u_e is selected as

$$u_e = \hat{f}_2 + K_P\eta + \gamma_2, \tag{23}$$

with $K_P > 0$ a gain matrix and $\hat{f}_2(x_2)$ an estimate of the unknown function $f_2(x_2)$. The signal $\gamma_2(t)$ is required to compensate for the mismatch between $\hat{f}_2(x_2)$ and $f_2(x_2)$, and is defined as (see [2])

$$\gamma_2 = \frac{\eta\rho_2^2}{\| \eta \| \rho_2 + \varepsilon_2}, \tag{24}$$

where ε_2 is a small, positive constant controller gain, the bounding positive scalar function ρ_2 is defined as

$$\rho_2 > \| \tilde{f}_2 \| = \| f_2 - \hat{f}_2 \|, \tag{25}$$

where the function approximation error $\tilde{f}_2$ is given by

$$\tilde{f}_2 = f_2 - \hat{f}_2. \tag{26}$$

Substituting (24) into the open loop dynamics of expression (15), the closed-loop current perturbation dynamics forms

$$L\dot{\eta} = \bar{f}_2(x_2) - K_p\eta. \quad (27)$$

The third step is the design of the fuzzy control $\bar{f}_{art}$ for the system of expression (18). It is important to note that this controller also serves as on-line reactive planner.

3.2 Fuzzy control

we develop a general design procedure consisting of selection of membership functions and establishment of a rule base for low level two-input/one output fuzzy logic controller, where the rule base has thirty rules.

3.2.1 Fuzzification

The fuzzy controller has two inputs: one is the distance d which is the minimum distance between the end-effectors of the robot and the nearest obstacle, and another is the position error e. The d mesure can be completed by a lot of distance measure system such as ultrasonic sonar system. The output of each fuzzy logic controller is the torque $\bar{F}_{art}$, which is required to be bounded $|\bar{F}_{art}| < \infty$.

The position error e is partitioned into five fuzzy sets: big negative (BN), small negative (SN), zero (Z), small positive (SP), and big positive (BP). Its fuzzy membership functions are symmetric and shown in Fig.2 (a).

The distance d consists of six fuzzy sets: far left (FL), left (L), close left (CL), close right (CR), right (R), and far right (FR). Its fuzzy membership functions are asymmetric and shown in Fig. 2 (b), where δ is the maximum ultrasonic range (if the ultrasonic sonar system is used to measure distance d).

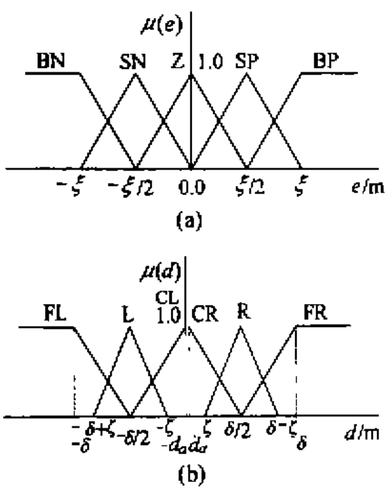

Fig. 2 Fuzzy membership functions

3.2.2 Rule base

The rule base is generalized as

R^i: If $e(k)$ is $\mu_1^i(e(k))$ and $\cdots$ and $e(k-n+1)$ is $\mu_n^i(e(k-n+1))$ and $d(k)$ is $\mu_1^i(d(k))$ and $\cdots$ and $d(k-m+1)$ is $\mu_m^i(e(k-m+1))$, then $F_i(k+1)$ is r. (28)

Our thirty rule bases are arranged into a look-up table with two inputs $\mu(d)$ and $\mu(e)$ fuzzy sets. The outputs of the base are F_j which describe the torque output and they are partitioned into 9 fuzzy sets: left very big (LVB), left big (LB), left small (LS), left very small (LVS), zero (Z), right very small (RVS), right small (RS), right big (RB), and right very big (RVB). For example, the rule 1 is

R^1: If d is FL and e is BN,
then F_i is LS. (29)

3.2.3 Defuzzification

For each of controllers, the following defuzzification formula is used.

$$\bar{F}_{art} = \sum_{i=1}^{n} F_i w^i / \sum_{i=1}^{n} w^i,$$

$$w^i = \prod_{p=1}^{n} \mu_p^i(e(k-p+1)) \times \prod_{h=1}^{n} \mu_h^i(d(k-h+1)). \quad (30)$$

The sign of the torque $\bar{F}_{art}$ gives the orientation of the link displacement, for example, for a planar robot, when $\bar{F}_{art}$ is positive, the link moves to the left, and when it is negative, the link moves to the right. The magnitude of this torque provokes the acceleration and deceleration motion of the link.

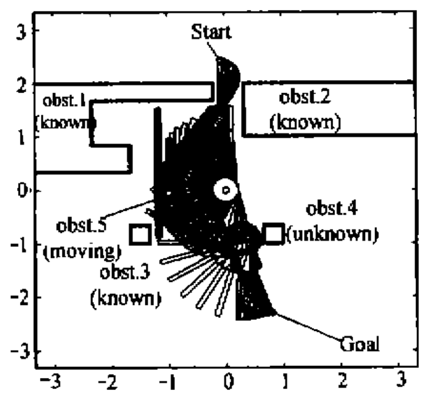

Fig. 3 Robot navigation with moving and unknown obstacles

4 Simulations and conclusions

Let $\xi = l_1 + l_2 = 2.3$m, $\delta = 2.8$m, $\zeta = 0.4$m, and $d_a = 20$mm, by adding moving and unknown obstacles, choosing the initial and desired joint angles as $q_1(0) =$

$91.6732(°), q_2(0) = 5.7296(°), q_{d_1} = -73.5211(°)$, $q_{d_2} = 11.4592(°)$, and keeping the other simulation parameters of the case 1, the following simulation (Fig.3) has been obtained. The robot successfully completes a complex manoeure avoiding moving, unknown and stationary obstacles. In the case of the moving obstacle, which has a constant velocity, the manipulator automatically reduces its velocity to avoid collision. This phenomenon shows the effective intelligent capability of the proposed motion-planning algorithm to deal with moving and unknown obstacles.

The simulation results (Fig.4) show the joint angle, the joint velocity, and the position error, as well as the distance between lower arm and the nearest obstacle.

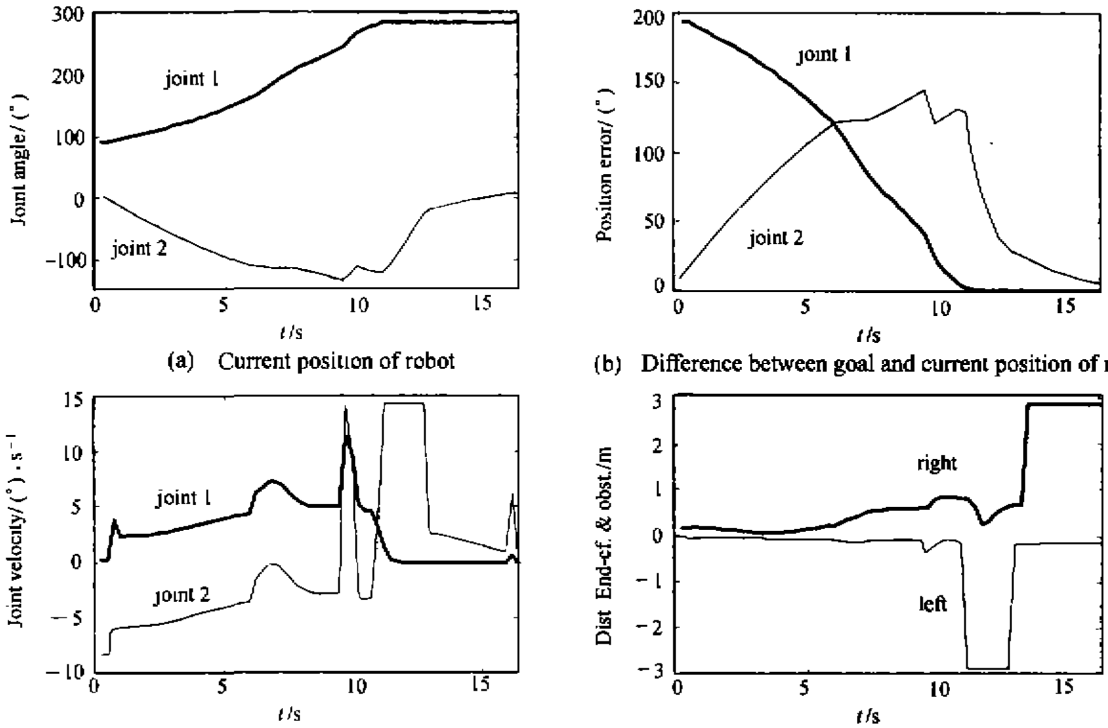

(a) Current position of robot (b) Difference between goal and current position of robot

(c) Joint velocity of each link (d) Distance d between robot and obstacles

Fig. 4 Simulation result

A new intelligent motion control strategy that makes possible the integration of robust and fuzzy control has been proposed for autonomous navigation of RLED robot manipulators. With the help of its "brain" (fuzzy-decision) which makes decisions about any action of the robot, it is shown that the robot autonomously reaches its target without collision with unknown or moving obstacles in an unstructured W-space where no trajectory is planned in advance. The close loop control system of fuzzy and robust is stable. This brings a high level of autonomy to the overall system, and makes use of the controller very attractive for real-time fast and nonstop sensor-based guidance of intelligent robot manipulators.

References

[1] Cheung E and Lumelsky V J. A sensitive skin system for motion control of robot arm manipulators [J]. Journal of Robotics and Autonomous Systems, 1992,10(1):9-32

[2] Dawson D M, Qu Z and Carrol J J. Tracking control of rigid-link electrically-driven robot manipulators [J]. Int. J. Control, 1992,56(5):991-1006

[3] Ding H and Li H X. Fuzzy avoidance control strategy for redundant manipulators [J]. Eng. Applications of Artificial Intelligence, 1999, 12(4):513-521

[4] Kwan C, Lewis F L and Dawson D M. Robuts neural-network control of rigid-link electrically driven robots [J]. IEEE Trans. Neural Networks, 1998,9(4):581-588

[5] Murray R M, Li Z and Sastry S S. A Mathematical Introduction to Robotic Manipulation [M]. Boca Raton: CRC Press,1994

[6] Qu Z and Dawson D M. Robust Tracking Control of Robot Manipulators [M]. New York: IEEE Press,1996

[7] Tam T J, Bejczy A K, Yun X, et al. Effect of motor dynamics on nonlinear feedback robot arm control [J]. IEEE Trans. Robotics Automat., 1991,7(1):114-122

(Continued on page 881)

work well with traditional single feedback loop. The (CGPC) algorithm developed in this paper is useful for this control problem. The running results of Biaxial film production process control system show the CGPC is effective for complex industrial control processes.

References

[1] Dumont G A. Application of advanced control methods in the pulp and paper industry — A survey [J]. Automatica, 1986, 22(1): 143 – 150

[2] Featherstone A P and Braatz R D. Control-oriented modeling of sheet and film processes [J]. AIChE. J., 1997, 43(8): 1989 – 2001

[3] Dave P, Willig D A, Kudva G K, et al. LP method in MPC of large-scale systems: application to papermachine CD control [J]. AIChE. J., 1997, 43(4): 1016 – 1031

[4] Clarke D W, Mohtadi C and Tuffs P S. Generalized predictive control, Part 1: The basic algorithm; Part 2: Extension and interpretations [J]. Automatica, 1989, 23(1): 137 – 160

[5] Clarke D W. Application of generalized predictive control to industrial processes [J]. IEEE Control System Magazine, 1988, 4(1): 49 – 55

[6] Richalet J. Industrial applications of model based predictive control [J]. Automatica, 1983, 29(10): 1251 – 1274

[7] Xi Y G. Predictive Control [M]. Beijing: National Defense Press, 1994

[8] Wang Liang and Langari Reza. Variable forgetting factor RLS algorithm with application to fuzzy time-varying systems identification [J]. Int. J. of Systems Science, 1996, 27(2): 205 – 214

本文作者简介

李少远 见本刊 2001 年第 2 期第 170 页.

席裕庚 见本刊 2001 年第 2 期第 170 页.

陈增强 1964 年生. 1997 年在南开大学计算机与系统科学系获得博士学位, 现为南开大学计算机与系统科学系教授. 研究领域为自适应预测控制、智能控制等的理论、方法与应用.

袁著祉 1937 年生. 毕业于南开大学数学系, 现为南开大学计算机与系统科学系教授, 博士生导师. 研究领域为自适应预测控制, 计算机控制系统与网络等.

(Continued from page 875)

[8] Bergluis H. Model-based robot control: from theory to practice [D]. Enschede, The Netherlands: University of Twente, 1993

[9] Wu wei, Jean B M and Zhang Qisen. Fuzzy sensor-based motion control among dynamic obstacles for intelligent rigid-link electrically driven arm manipulators [J]. Journal of Intelligent and Robotic system (Kluwer), 2001, 30(1): 1 – 23

[10] Kim J O and Khosla P K. Real-time obstacle avoidance using harmonic potential functions [J]. IEEE Trans. Robotics and Automation, 1992, 8(3): 338 – 349

本文作者简介

魏 武 1970 年生, 博士. 现任教于长沙交通学院, 并在清华大学自动化系从事博士后研究工作. 国际 IEEE 控制系统、汽车技术、信号处理、系统人和控制系统、机器人和自动化协会会员. 已被 Automatica, International Journal of Intelligent and Robotics Systems 等国际期刊和国际会议录取论文近 30 余篇. 研究兴趣: 机器人运动控制和规划, 智能交通系统, 模式识别, 计算机视觉, 图像处理和智能控制等.

Jean Bosco Mbede 1966 年生, 现为华中科技大学控制科学与工程系博士. 发表学术论文 20 余篇, 主要研究方向为: 机器人运动控制和规划, 模式识别和智能控制等.

黄心汉 1946 年生, 现为华中科技大学控制科学与工程系教授, 博士生导师、智能与控制工程研究所所长, 兼任中国人工智能学会智能机器人学会副理事长等职.